The Effect of Eddy–Eddy Interactions on Jet Formation and Macroturbulent Scales

REI CHEMKE AND YOHAI KASPI

Department of Earth and Planetary Sciences, Weizmann Institute of Science, Rehovot, Israel

(Manuscript received 16 December 2015, in final form 22 February 2016)

ABSTRACT

The effect of eddy–eddy interactions on zonal and meridional macroturbulent scales is investigated over a wide range of eddy scales, using high-resolution idealized GCM simulations with and without eddy–eddy interactions. The wide range of eddy scales is achieved through systematic variation of the planetary rotation rate and thus multiple-jet planets. It is found that not only are eddy–eddy interactions not essential for the formation of jets, but the existence of eddy–eddy interactions decreases the number of eddy-driven jets in the atmosphere. The eddy–eddy interactions have little effect on the jet scale, which in both types of simulations coincides with the Rhines scale through all latitudes. The decrease in the number of jets in the presence of eddy–eddy interactions occurs because of the narrowing of the latitudinal region where zonal jets appear. This narrowing occurs because eddy–eddy interactions are mostly important at latitudes poleward of where the Rhines scale is equal to the Rossby deformation radius. Thus, once eddy–eddy interactions are removed, the conversion from baroclinic to barotropic eddy kinetic energy increases, and eddy–mean flow interactions intrude into these latitudes and maintain additional jets there. The eddy–eddy interactions are found to increase the energy-containing zonal scale so it coincides with the jets' scale and thus make the flow more isotropic. While the conversion scale coincides with the most unstable scale, the Rossby deformation radius does not provide a good indication to these scales in both types of simulations.

1. Introduction

The turbulent behavior of large scales in the atmosphere suggests the importance of eddy–eddy and eddy–mean flow interactions in controlling the atmospheric energy spectrum. In particular, studying their effect on the energy-containing scales in the atmosphere is crucial for developing a better understanding of the physical processes at synoptic scales.

The two-dimensional turbulence character of the atmosphere (e.g., Charney 1971; Baer 1972; Boer and Shepherd 1983; Nastrom and Gage 1985; Shepherd 1987b) suggests that eddy–eddy interactions should have an important role in the dynamics. Rhines (1977) and Salmon (1978) argued that, as energy is converted from the baroclinic to barotropic mode at the Rossby deformation radius (a scale that linear theory predicts is proportional to the most unstable wavelength; Eady 1949), it can inverse cascade in the barotropic mode to large scales through eddy–eddy interactions. The inverse cascade will halt at the Rhines scale because of the opposite dependence of frequency on wavenumber in the turbulent and Rossby waves regimes (Rhines 1975; Holloway and Hendershott 1977; Rhines 1979; Danilov and Gurarie 2000; Galperin et al. 2006; Kaspi and Flierl 2007). Nonetheless, the inverse energy cascade continues up to the zero zonal wavenumber, and formation of zonal jets occurs (e.g., Rhines 1977; Williams 1978; Rhines 1994), with a meridional wavenumber following the Rhines scale (Rhines 1975; Vallis and Maltrud 1993; Panetta 1993; Lee 2005; Kaspi and Flierl 2007; O'Gorman and Schneider 2008b; Chemke and Kaspi 2015b). When the ratio (scale separation) between the Rhines scale and the Rossby deformation radius, which follows the quasigeostrophic (QG) supercriticality (Held and Larichev 1996), is greater than one, eddy–eddy interactions are dominant and an inverse energy cascade occurs (Chemke and Kaspi 2015b). Interestingly, in both QG models (Larichev and Held 1995) and idealized global circulation models (GCMs) (Chemke and Kaspi 2015b), the Rossby deformation radius was not found to

Corresponding author address: Rei Chemke, Department of Earth and Planetary Sciences, Weizmann Institute of Science, 234 Herzl St., Rehovot, Israel 7610001.
E-mail: rei.chemke@weizmann.ac.il

DOI: 10.1175/JAS-D-15-0375.1

coincide with the conversion scale of baroclinic to barotropic kinetic energy.

The lack of a clear scale separation between the Rhines scale and the deformation radius and the fact that an inverse energy cascade, associated with two-dimensional turbulence, is not observed in the atmosphere (e.g., Baer 1972; Boer and Shepherd 1983; Nastrom and Gage 1985) have raised questions regarding the significance of eddy–eddy interactions (Panetta 1993; Schneider and Walker 2006; Farrell and Ioannou 2007; O'Gorman and Schneider 2007; Constantinou et al. 2014; Marston 2012; Srinivasan and Young 2012; Bakas and Ioannou 2014). In the absence of such scale separation (supercriticality is equal to or smaller than one), the eddy–eddy interactions should be negligible in the balance, implying that the Rossby deformation radius should follow the energy-containing wavenumber (Schneider and Walker 2006; O'Gorman and Schneider 2008b; Merlis and Schneider 2009) and the width of the jet (Schneider and Walker 2006). This implies the major role of eddy–mean flow interactions in maintaining the jets (Shepherd 1987b; Huang and Robinson 1998; Farrell and Ioannou 2007) and in adding energy at large scales through a shear-induced spectral transfer (e.g., Shepherd 1987b; Huang and Robinson 1998). Indeed, several studies showed that the spectral slope of the kinetic energy and the energy-containing wavenumber remain the same in simulations without eddy–eddy interactions (O'Gorman and Schneider 2007; Chai and Vallis 2014), as does the meridional structure of the jets (Tobias et al. 2011; Constantinou et al. 2014; Marston 2012; Srinivasan and Young 2012; Tobias and Marston 2013; Bakas and Ioannou 2014).

On the other hand, other studies have shown that the supercriticality could vary above one (Zurita-Gotor 2008; Jansen and Ferrari 2012, 2013; Chai and Vallis 2014). Thus, nonlinear eddy–eddy interactions become important (Zurita-Gotor and Vallis 2009; Jansen and Ferrari 2012; Chai and Vallis 2014; Chemke and Kaspi 2015b), and the energy-containing wavenumber coincides with the Rhines scale (Jansen and Ferrari 2012; Chai and Vallis 2014; Chemke and Kaspi 2015b). At large supercriticality the energy-containing wavenumber does not correlate between simulations with and without eddy–eddy interactions (Chai and Vallis 2014). Moreover, several studies observed an increase in the number of jets (the meridional energy-containing wavenumber) as the eddy–eddy interactions were removed (O'Gorman and Schneider 2007; Chai and Vallis 2014; Ait-Chaalal and Schneider 2015).

In Chemke and Kaspi (2015b), we showed the presence of a critical latitude where the Rhines scale is equal to the Rossby deformation radius. Poleward of this latitude, the Rhines scale is larger than the Rossby deformation radius, and the QG supercriticality is larger than one. Hence, here we refer to this latitude as the supercriticality latitude. Poleward of this latitude, the length scale of the energy-containing zonal wavenumber coincides with the width of the jet and the Rhines scale, and the eddy–eddy interactions play an important role in transferring energy both upscale and downscale. Equatorward of the supercriticality latitude, the eddy–mean flow interactions become dominant and the energy-containing zonal scale was found to be larger than the jets and Rhines scales.

In this study, we examine the importance of the eddy–eddy interactions in controlling the macroturbulent scales. Because of their latitudinal dependence (Chemke and Kaspi 2015b), we study their effect by comparing simulations with and without eddy–eddy interactions as a function of latitude. The eddy–eddy interactions are found to decrease the number of eddy-driven jets in the atmosphere, without altering their width, by narrowing the region where these jets appear. Consistently, both the conversion from baroclinic to barotropic eddy kinetic energy (EKE) and eddy–mean flow interactions decrease, especially at high latitudes, where the eddy–eddy interactions are found to be important. While the eddy–eddy interactions have a minor effect on the Rhines and jets' scales, they tend to increase both the energy-containing scale (so it would equal the width of the jet), and the energy-conversion scale.

Section 2 describes the idealized GCM and presents briefly the formulation of the quasi-linear (QL) simulations. Sections 3 and 4 discuss the effect of eddy–eddy interactions on the jet and macroturbulent scales, respectively, by comparing results from simulations with and without eddy–eddy interactions. The results are summarized in section 5.

2. Model

We use an idealized aquaplanet moist GCM based on the GFDL Flexible Modeling System (FMS). This is a spherical coordinate primitive equation model of an ideal-gas atmosphere similar to that in Frierson et al. (2006) and O'Gorman and Schneider (2008a) and to what we have used in Chemke and Kaspi (2015a,b). The lower layer of the model is an ocean slab that has no dynamics but only exchanges energy with the lowest atmospheric layer. Simplified Monin–Obukhov similarity theory is used to calculate both the surface drag coefficient for the calculation of surface stress and the diffusion coefficients within the boundary layer (Frierson et al. 2006). Shortwave radiation is imposed

as a perpetual equinox, and longwave radiative transfer is represented by a two-stream gray radiation scheme (Goody 1964; Held 1982).

To examine the effect of the nonlinear eddy–eddy interactions on macroturbulent scales, we remove these interactions from the momentum and temperature equations (O'Gorman and Schneider 2007). We refer to these simulations as the QL simulations and to the simulations with eddy–eddy interactions as the full simulations. The zonal mean temperature and momentum equations are similar in the QL and full simulations, as they both contain all the mean–mean flow interactions (i.e., interactions involving only the zero zonal wavenumber), and the eddy–mean flow interactions, which include only the contributions of the mean eddy fluxes [e.g., $\overline{v'(\partial u'/\partial y)}$, where u and v are the zonal and meridional velocities and the bar and prime denote zonal mean and deviation from this mean, respectively]. However, the eddy equations differ in the full and QL simulations as the purely eddy interactions {e.g., $[v'(\partial u'/\partial y)]'$, which involve in the energy equation triad interactions among three different zonal wavenumbers} are removed in the QL simulations. In this way, the spectrum is built only through eddy–mean flow interactions.

We carry out a set of simulations where we systematically increase the planetary rotation rate up to 8 times Earth's rotation rate Ω_e. Increasing the rotation rate enables us to study multiple-jet planets at all latitudes (because of the poleward migration of the eddy-driven jets; Chemke and Kaspi 2015a) and thus to accumulate better statistics on the meridional and zonal containing scales. At high rotation rates, the eddy length scale is relatively small compared to the planet size (e.g., Schneider and Walker 2006; Kaspi and Showman 2015), which provides a wide separation among the important macroturbulence scales (the Rhines scale, Rossby deformation radius, scale of barotropic to baroclinic energy conversion, etc.). Each simulation has 30 vertical sigma layers (pressure normalized by the surface pressure) at T170 horizontal resolution (0.7° × 0.7°). Unless otherwise stated, the results represent the time average of the last 500 days of 2000-day simulations.

3. The width of the jets

As discussed in section 1, previous studies (O'Gorman and Schneider 2007; Chai and Vallis 2014) showed that, in Earthlike simulations when the eddy–eddy interactions were removed, the jets were compressed toward the equator and an additional jet emerged at higher latitudes. Figure 1 shows a snapshot of the meridional–height cross section of the mean zonal wind in the full and QL $8\Omega_e$ simulations. Similar to the results of Tobias and Marston (2013), the mean zonal wind intensifies in the QL simulation, particularly at high latitudes, as in Marston (2012). To see how robust this phenomenon is, we calculate the number of eddy-driven jets[1] through a series of simulations with different rotation rates (Fig. 2a). As the rotation rate increases, the eddy length scale decreases, which increases the number of jets in the atmosphere (e.g., Williams and Holloway 1982; Navarra and Boccaletti 2002; Kaspi and Schneider 2011; Chemke and Kaspi 2015a), since their meridional scale correlates with the Rhines scale (Rhines 1975; Vallis and Maltrud 1993; Panetta 1993; Lee 2005; O'Gorman and Schneider 2008b; Chemke and Kaspi 2015b). The number of the eddy-driven jets in the QL simulations (red dots in Fig. 2a) is larger by ~58% than in the full simulations (blue dots in Fig. 2a). This can also be seen by observing the mean zonal wind in the full and QL $8\Omega_e$ simulations (Fig. 1).

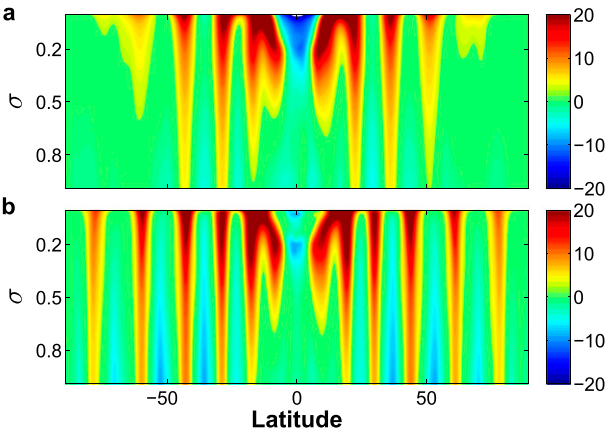

FIG. 1. Snapshot of the mean zonal wind (m s^{-1}) as a function of sigma and latitude for the $8\Omega_e$ simulations (a) with and (b) without eddy–eddy interactions.

The presence of eddy-driven jets in the QL simulations at latitudes where these jets were absent in the full simulations (Fig. 1) implies that the production of the zonal jets through local processes in spectral space of nonlinear eddy–eddy interactions (e.g., Rhines 1977; Williams 1978; Rhines 1994) is less important in such

[1] We define an eddy-driven jet to be where its maximum vertical and zonal average velocity is larger than 50% of the maximum vertical and zonal average velocity of the strongest jet. This avoids low values of zonal wind for the calculation of the number of eddy-driven jets. The results are not sensitive to taking a lower or higher percentage. Defining an eddy-driven jet as a local maximum of the zonal wind that resides in the baroclinic zone (e.g., the latitudinal extent of the baroclinic zone is defined where 30% of the maximum value of the eddy heat flux is observed near the surface; Schneider and Walker 2006), produces the same results.

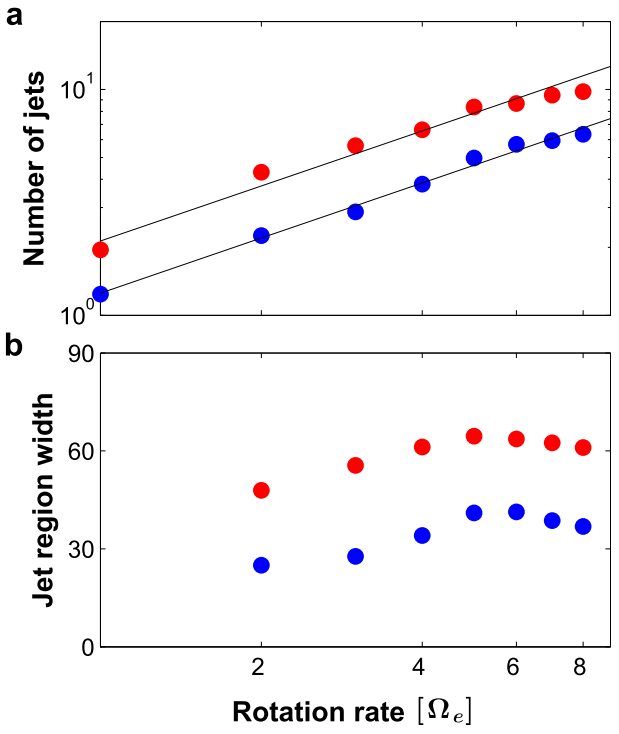

FIG. 2. (a) The number of eddy-driven jets in both hemispheres as a function of rotation rate, for simulations with (blue) and without (red) eddy–eddy interactions. (b) The latitudinal width of the jet region for simulations with (blue) and without (red) eddy–eddy interactions. The two black lines in (a) follow $C_{1,2}\Omega^{0.81}$, where $C_1 = 1.58C_2$. The width of the jet region is defined as the distance between the most equatorward and poleward eddy-driven jets. Only simulations where the eddy-driven jets are clearly separated are taken into account for the analysis of (b) ($\Omega > \Omega_e$).

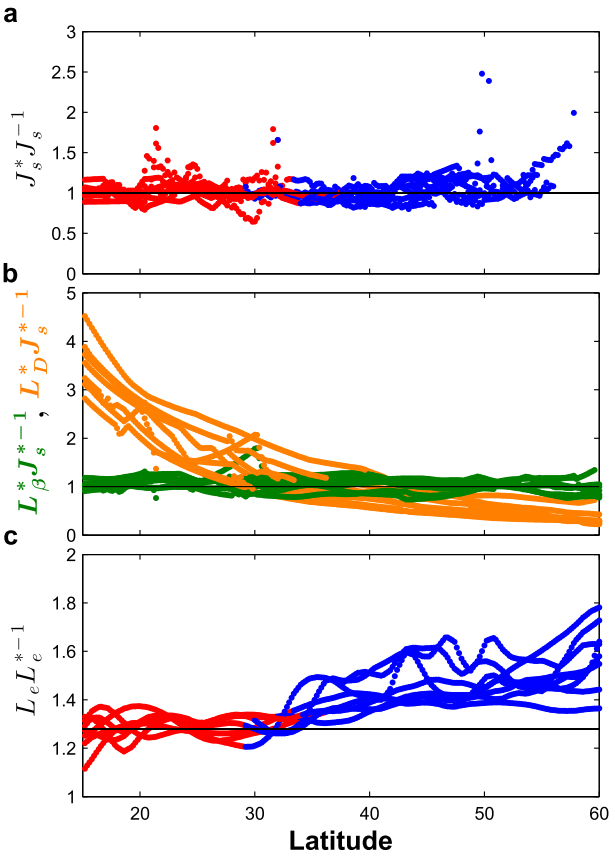

FIG. 3. Scale properties as a function of latitude for all rotation rates. Each dot represents a ratio at a single latitude and rotation rate. (a) The ratio between the width of the jets in the QL (denoted with an asterisk) and full simulations. (b) The ratio between the Rhines scale and the width of the jet (green) and between the Rossby deformation radius and the width of the jet (orange) in the QL simulations. (c) The ratio between the length scale of the energy-containing zonal wavenumber, calculated from the zonal spectrum of the barotropic eddy meridional velocity [Eq. (7)] in the full and QL (denoted with an asterisk) simulations. In (a) and (c) the blue (red) dots represent latitudes poleward (equatorward) of the supercriticality latitude.

atmospheric simulations (e.g., Farrell and Ioannou 2007; Constantinou et al. 2014; Marston 2012; Srinivasan and Young 2012). The maintenance of jets by eddy–mean flow interactions (e.g., Shepherd 1987b; Panetta 1993; Huang and Robinson 1998; Robinson 2006; Farrell and Ioannou 2007) is further discussed in the next section.

O'Gorman and Schneider (2007) suggested that the meridional wavenumber of the mean flow is smaller in the full simulation because of the tendency of eddy–eddy interactions to inverse cascade energy near the zero zonal wavenumber to smaller meridional wavenumbers. This could imply a narrowing of the jet's width as the eddy–eddy interactions are removed. However, as in Constantinou et al. (2014) and Srinivasan and Young (2012), when the eddy–eddy interactions are removed in our simulations, the width of the jet remains similar to the width of the jet in the full simulations (95% of the jets either increased or decreased their width by less than 20%) through all latitudes and rotation rates (Fig. 3a). The width of the jet is defined as the meridional distance between two consecutive minima values of the mean zonal wind.

The increase in the number of eddy-driven jets in the QL simulations (Fig. 2a) is because of an increase in the latitudinal width of the region where these jets appear (Fig. 2b). We refer to this region as the "jet region." By comparing the mean zonal wind for the QL and full $8\Omega_e$ simulations (Fig. 1), the jet region becomes wider (stronger eddy-driven jets appear at higher latitudes) as the eddy–eddy interactions are removed. This increase in the width of the jet region is found to occur through all rotation rates (Fig. 2b). The latitudinal jet region increases in the QL simulations (red dots in Fig. 2b) on average by ~70% compared to the full simulations (blue dots in Fig. 2b). Hence, most of the change in the meridional structure of the zonal wind in the QL simulations comes from the expansion of the jet region (Fig. 1b), and not from a

change in the jets' width (Fig. 3a). The increase in the QL simulations of the jet region (~70%) is larger than the increase in the number of eddy-driven jets (~58%), since the jets that appear at higher latitudes are wider (Fig. 1) because of the latitudinal dependence of the Rhines scale (Huang and Robinson 1998; Kidston and Vallis 2010; Chemke and Kaspi 2015a,b).

The width of the jet region displays a nonmonotonic dependence on rotation rate in both full and QL simulations. For the lower rotation rates, the jet region increases with rotation rate (Fig. 2b) mainly because of the decrease in the latitudinal extent of the Hadley cell (Held and Hou 1980; Walker and Schneider 2006). On the other hand, at higher rotation rates, the jet region slowly decreases with rotation rate, which might be because of the weakening of the poleward eddy heat flux with rotation rate (Hunt 1979; Kaspi and Showman 2015), which limits the edge of the baroclinic and jet regions.

The width of the jets in the QL simulations is found to scale with the Rhines scale and not with the Rossby deformation radius (Fig. 3b) through all latitudes and rotation rates, as was shown to occur in the full simulations as well (Chemke and Kaspi 2015b). The Rhines scale is defined as

$$L_\beta = 2\pi\left[\frac{(\mathrm{EKE})^{1/2}}{\beta}\right]^{1/2}, \tag{1}$$

where EKE is the vertically averaged eddy kinetic energy. The eddies are defined as a deviation from the zonal mean, and β is the meridional derivative of the Coriolis parameter f. The Rossby deformation radius is defined as

$$L_D = 2\pi\frac{NH}{f}, \tag{2}$$

where H is the tropopause height calculated as the height where the static stability reaches a threshold value of $0.015\,\mathrm{s}^{-1}$, and $N = [(g/\vartheta)(\partial\vartheta/\partial z)]^{1/2}$ is the vertically averaged static stability below the tropopause height [similar to Frierson et al. (2006)], where g is gravity, z is height, and ϑ is the potential temperature.[2]

The conversion between wavenumbers k and length scales L is computed at each latitude θ as follows:

$$L = \frac{2\pi a\cos(\theta)}{k}, \tag{3}$$

where a is Earth's radius.

The correlation of the width of the jet and the Rhines scale, latitude by latitude through all rotation rates, in the QL simulations implies that the width of the jet cannot be determined by an inverse energy-cascade argument through eddy–eddy interactions. Similarly, in the full simulations, where eddy–eddy interactions were found to be weak (equatorward of the supercriticality latitude), the jets' width correlates with the Rhines scale. While the above correlation in the QL simulations occurs similarly at all latitudes (Fig. 3b), in the full simulations the width of the jet coincides better with the Rhines scale poleward of the supercriticality latitude, where eddy–eddy interactions were found to be important [see Fig. 8d in Chemke and Kaspi (2015b)]. This suggests that the eddy–eddy interactions do have some effect on the width of the jet, mostly poleward of the supercriticality latitude. Nonetheless, as the ratio between the width of the jets in the full and QL simulations behaves similarly poleward (blue dots in Fig. 3a) and equatorward (red dots in Fig. 3a) of the supercriticality latitude, this effect may be of less importance.

4. Macroturbulent scales

The effect of eddy–eddy interactions on the meridional structure of the flow can be further understood by comparing the different components in the budget of the zonal barotropic EKE [following the analysis of Larichev and Held (1995), but here as a function of latitude, as in Chemke and Kaspi (2015b)]. Even though the meridional structure of the mean flow and eddies are also affected by meridional macroturbulent scales (Simmons 1974; Vallis and Maltrud 1993; Huang and Robinson 1998; Huang et al. 2001; Barry et al. 2002), here we study the effect of eddy–eddy interactions on the meridional structure of the jets using the zonal spectrum; this is done mainly because of two reasons. First, this allows for studying the effect of eddy–eddy interactions as a function of latitude (both poleward and equatorward of the supercriticality latitude). Second, the eddy–eddy interactions also have a latitudinal effect on other zonal macroturbulent scales (e.g., the baroclinic conversion and energy-containing scales), which

[2] The Rossby deformation radius is similar to the Rossby deformation radius calculated when applying the WKBJ approximation on the eigenvalue problem for the vertical structure of the QG streamfunction (Gill 1982; Chelton et al. 1998). The 2π factor represents the conversion to wavelength. Rhines scales calculated using the barotropic EKE (e.g., Haidvogel and Held 1980; Schneider and Walker 2006; Jansen and Ferrari 2012; Chai and Vallis 2014), the energy-cascade rate (Held and Larichev 1996), or the Rayleigh–Kuo stability criterion (Farrell and Ioannou 2007) were found to be less consistent with the width of the jet and with the halting scale of the inverse energy cascade (Chemke and Kaspi 2015b) than the Rhines scale in Eq. (1).

are further analyzed below. The zonal spectral barotropic EKE is computed using a one-dimensional Fourier analysis for each latitude (Saltsman 1957) as follows:

$$\mathrm{bEKE}_k = \langle |[u]'_k|^2 + |[v]'_k|^2 \rangle, \tag{4}$$

where angle brackets denote a time mean and square brackets denote a vertical average.[3] The subscript k denotes the zonal spectral components with a zonal wavenumber k.

Two components of the budget of the barotropic EKE are presented in Fig. 4: the conversion of baroclinic EKE to barotropic EKE,

$$\mathrm{CT} = \left\langle \mathrm{Re}\left\{ -[u]^*_k \left([\mathbf{u}^+ \cdot \nabla u^+]'_k - \left[\frac{u^+ v^+ \tan\theta}{a} \right]'_k \right) - [v]^*_k \left([\mathbf{u}^+ \cdot \nabla v^+]'_k + \left[\frac{u^+ u^+ \tan\theta}{a} \right]'_k \right) \right\} \right\rangle, \tag{5}$$

and the eddy–mean flow interactions,

$$\mathrm{EM} = \left\langle \mathrm{Re}\left(-[u]^*_k \left\{ (\overline{[\mathbf{u}]} \cdot \nabla [u]')_k + ([\mathbf{u}]' \cdot \nabla \overline{[u]})_k - \left(\frac{\overline{[u]}[v]' \tan\theta}{a} \right)_k - \left(\frac{[u]'\overline{[v]} \tan\theta}{a} \right)_k \right\} - [v]^*_k \left\{ (\overline{[\mathbf{u}]} \cdot \nabla [v]')_k + ([\mathbf{u}]' \cdot \nabla \overline{[v]})_k + 2\left(\frac{\overline{[u]}[u]' \tan\theta}{a} \right)_k \right\} \right) \right\rangle, \tag{6}$$

where $\mathbf{u}$ denotes the three-dimensional velocity vector, the asterisk denotes a complex conjugate, and the plus sign superscript denotes deviation from vertical average. Note that the conversion from baroclinic to barotropic may contain the conversions from all baroclinic modes and not only from the first baroclinic mode, as occurs in the classic two-layer model (e.g., Salmon 1978). The above components are presented only for the $8\Omega_e$ simulation, as it captures the properties both above and below the supercriticality latitude (Fig. 4). A similar analysis was conducted in previous studies (e.g., Lambert 1984; Koshyk and Hamilton 2001; Jansen and Ferrari 2012; Chai and Vallis 2014), only for the EKE using two-dimensional spectra. The black line in Fig. 4 shows the supercriticality latitude from the full simulation, where the Rhines scale [blue line; Eq. (1)] is equal to the Rossby deformation radius [white line; Eq. (2)]. The gray line shows the conversion from baroclinic to barotropic EKE zonal wavenumber, calculated as the centroid of Eq. (5). This definition provides conversion wavenumbers that are closest to the maximum of Eq. (5).

It has been suggested that the presence of eddy–eddy interactions reduces the conversion of potential to kinetic energy, which can explain the increase in the kinetic energy in the QL simulations (e.g., O'Gorman and Schneider 2007; Chai and Vallis 2014). In the QL simulations, the conversion from baroclinic to barotropic EKE indeed strengthens (the maximum conversion is 1.6 times larger in the QL simulations, poleward of the supercriticality latitude), compared to the full simulations, mostly at intermediate scales (Berloff and Kamenkovich 2013a,b), while it weakens at large and small scales (cf. Figs. 4a,b). This is consistent with the increase of barotropic EKE in the QL simulations at intermediate scales and a decrease at large and small scales (Chemke and Kaspi 2015b). This opposite behavior at different scales might suggest that the mean EKE in the full and QL simulations is also similar. Indeed, the Rhines scale [computed using the EKE; Eq. (1)] is found to be similar for each rotation rate in the full and QL simulations (Fig. 5, blue dots). The increase in baroclinic conversion to the barotropic mode in the QL simulations is consistent with the tendency of the eddy–eddy interactions to make the stratification less uniform (not shown). A more uniform stratification, as occurs in the atmosphere compared to the ocean, enables a stronger baroclinic conversion (Fu and Flierl 1980; Smith and Vallis 2001, 2002; Chemke and Kaspi 2016).

The conversion from baroclinic to barotropic EKE not only strengthens but also shifts to larger zonal wavenumbers in the QL simulations and reaches higher latitudes (cf. gray line in Figs. 4a,b). The eddy–mean flow interactions also strengthen and intrude into higher latitudes in the QL simulations [replacing the strong eddy–eddy interactions poleward of the supercriticality latitude; Fig. 8d in Chemke and Kaspi (2015b)] and maintain the jets there (Figs. 1 and 4c,d). Thus, by weakening the baroclinic conversion and efficiently spreading it locally in spectral space, the eddy–eddy interactions inhibit jet formation at high latitudes. Not

[3] Studying the barotropic energy provides an understanding of the transfers of EKE to larger scales by both eddy–eddy and eddy–mean flow interactions (Rhines 1977; Salmon 1978). Thus, in order to study only the barotropic components, it is necessary to first take a vertical average and only then compute the deviation from zonal mean.

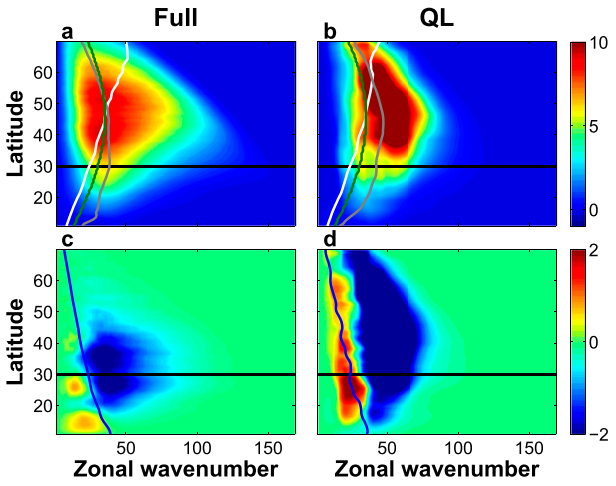

FIG. 4. Components of the barotropic EKE equation [10^{-5} m^2 s^{-3}; Eqs. (5) and (6)] in the $8\Omega_e$ run as a function of latitude and zonal wavenumber. A simulation (a),(c) with and (b),(d) without eddy–eddy interactions of (top) conversion of baroclinic EKE and (bottom) eddy–mean flow interactions. Each component is multiplied by the wavenumber and smoothed with a 20-point running mean. The colored lines correspond to the supercriticality latitude (where the Rhines scale is equal to the Rossby deformation radius) from the full simulation (black), the conversion wavenumber of baroclinic to barotropic EKE (gray), the Rhines scale (blue), the maximum baroclinic growth wavenumber (green), and the Rossby deformation wavenumber (white) (see text for definitions).

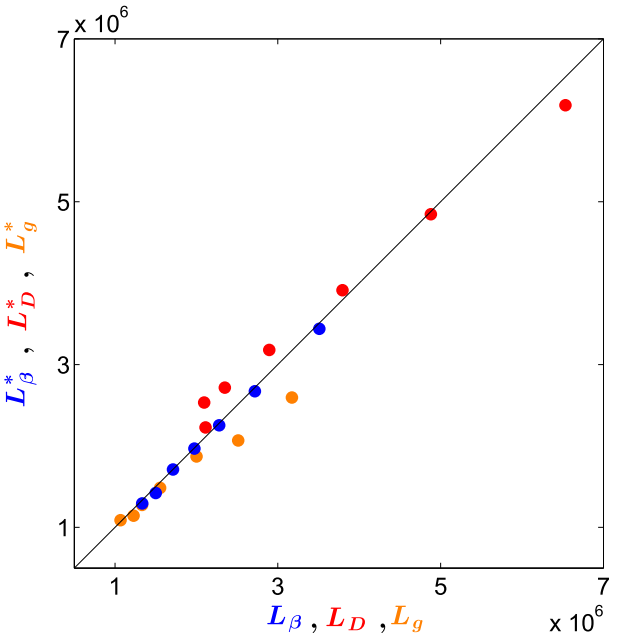

FIG. 5. The Rhines scale (blue), the Rossby deformation radius (red), and the conversion scale from baroclinic to barotropic EKE (orange) in the QL simulations (denoted with an asterisk), compared to the full simulations for all rotation rates. For comparing the scales in the QL and full simulations, the meridional average of each scale is taken over the jet region calculated from the full simulations (defined as the distance between the most equatorward and poleward jet).

only does the transfer of barotropic EKE to the mean flow increase in the QL simulation, but the addition of barotropic EKE to large scales from the mean flow also increases (Figs. 4c,d). While in the QL simulations, the addition of barotropic EKE by the eddy–mean flow interactions at large scales coincides with the Rhines scale (blue line, Fig. 4d), in the full simulations, on the other hand, the addition of barotropic EKE by eddy–eddy interactions coincides with the Rhines scale (Chemke and Kaspi 2015b).

In the QL simulations, as in the full simulations, the Rossby deformation radius does not coincide with the conversion scale of baroclinic to barotropic EKE (white and gray lines in Figs. 4a,b). This differs from the classic two-layer phenomenology of Salmon (1978) and can be more robustly seen in Fig. 5 by comparing the deformation radius (red) and conversion scale (orange) at each rotation rate simulation, where all scales decrease monotonically with rotation rate. At low rotation rates (larger scales in Fig. 5), both the conversion scale and the Rossby deformation radius are larger in the full simulations. At high rotation rates, on the other hand, while the conversion scale better coincides in the QL and full simulations (although still larger in the full simulation), the Rossby deformation radius is larger in the QL simulations (Fig. 5). The conversion scale decreases with rotation rate, as the inverse cascade of the barotropic EKE is being arrested at smaller Rhines scales (Chai and Vallis 2014).

The green line in Fig. 4 shows the scale of maximum baroclinic growth, which is the wavenumber corresponding to the fastest growth rate computed using a linear normal-mode instability analysis (Smith 2007). This is done by solving the linearized QG potential vorticity equation at each latitude using the meridional potential vorticity gradient, mean zonal wind, and density from the idealized GCM simulations. As in the filtering method of Smith (2007), in order to consider only the most unstable wavenumbers that are energetically important, we normalized the maximum growth rate of all levels by the eddy available potential energy (EAPE). The EAPE is estimated using the variance of the potential temperature field (e.g., Lorenz 1955; Saltsman 1957; Boer 1975; Schneider and Walker 2006).[4] Even

[4] Applying a shortwave cutoff at each latitude by filtering out the unstable wavenumbers where the conversion from baroclinic to barotropic EKE is less than 85% of the maximum conversion produces the same results.

though the Rossby deformation radius does not coincide with the conversion scale, the scale of maximum baroclinic growth does show a similar latitudinal behavior as the conversion scale, consistent with Jansen and Ferrari (2012), but here also through all latitudes (Figs. 4a,b). In the QL simulation, the conversion scale is smaller than the scale of maximum baroclinic growth (Fig. 4b), as in the full simulation equatorward of the supercriticality latitude, where eddy–eddy interactions are weaker (Fig. 4b). On the other hand, poleward of the supercriticality latitude in the full simulation, the scale of maximum baroclinic growth coincides with the conversion scale (Fig. 4a).

Similar to the meridional direction, the energy-containing zonal wavenumber also increases in the QL simulations (Fig. 3c). As in O'Gorman and Schneider (2008b) and Chemke and Kaspi (2015b), the energy-containing zonal wavenumber is computed using the "squared inverse centroid" of the zonal spectrum of the barotropic eddy meridional velocity as follows:[5]

$$k_e^2 = \frac{\sum_k |[v]'_k|^2}{\sum_k k^{-2} |[v]'_k|^2}. \tag{7}$$

The length scale of the energy-containing zonal wavenumber is not only larger in the full simulations [consistent with the QL simulations under strong supercriticality in Chai and Vallis (2014)], but also its ratio with the length scale of the energy-containing zonal wavenumber in the QL simulations increases with latitude (Fig. 3c, blue dots). Equatorward of the supercriticality latitude, the length scale of the energy-containing zonal wavenumber is found to be larger in the full simulations by a factor of ~1.3 (Fig. 3c, red dots). At these latitudes, the width of the jet is smaller than the length scales of the energy-containing zonal wavenumbers in both full and QL simulations (Fig. 6, red dots). On the other hand, poleward of the supercriticality latitude, the jet and energy-containing scales coincide only in the full simulations (Fig. 6, blue dots).

The effect of eddy–eddy interactions on the ratio between the zonal energy-containing and meridional width of the jets can be explained by the tendency of the eddy–eddy interactions to spread the barotropic EKE along lines of constant total wavenumbers

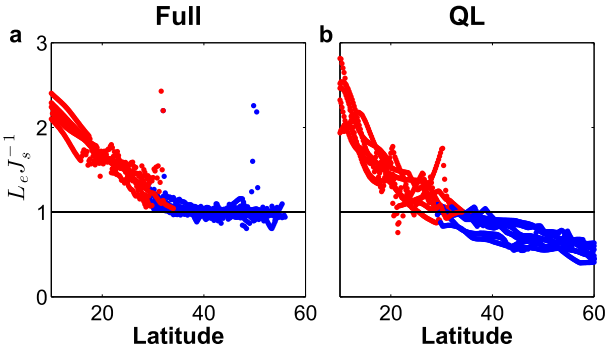

FIG. 6. The ratio of the length scale of the energy-containing zonal wavenumber, calculated from the zonal spectrum of the barotropic meridional velocity [Eq. (7)], and the jet space as a function of latitude for all rotation rates presented in Fig. 2b for simulations (a) with and (b) without eddy–eddy interactions. The blue (red) dots represent latitudes poleward (equatorward) of the supercriticality latitude.

(Fig. 7a, turbulence isotropization), as discussed in Shepherd (1987a) and Huang and Robinson (1998). In the QL simulation, the lack of eddy–eddy interactions reduces the isotropization of the flow, and the barotropic EKE is no longer spread along lines of constant total wavenumbers (Fig. 7b). As a result, the meridional width of the jet no longer coincides with the zonal energy-containing scale poleward of the supercriticality latitude (Fig. 6b, blue dots). Furthermore, the energy-containing wavenumber is isolated in the spectral space (Fig. 7b) once these interactions are removed.

5. Conclusions

In this study, we show that eddy–eddy interactions have a large effect on both the meridional and zonal structure of jets in a series of idealized GCM simulations where we systematically compare simulations with (full simulations) and without eddy–eddy interactions [quasi-linear simulations (QL)] at different rotation rates. The different rotation rates allow us to perform the analysis over a continuous range of latitudes, eddy scales, and jet widths. Our main conclusions are as follows:

- The eddy–eddy interactions are found to decrease the number and intensity of eddy-driven jets in the atmosphere (Figs. 1 and 2a), by limiting the latitudinal extent of the region where these jets appear (Fig. 2b). This implies not only that eddy–eddy interactions are not a prerequisite for the formation of zonal jets in the atmosphere, but also that they act to inhibit jet formation.
- Eddy–eddy interactions are found to limit the barotropization of the flow mostly poleward of the

[5] This definition produces an energy-containing zonal wavenumber closest to the peak of the zonal spectrum of the barotropic eddy meridional velocity, and its length scale [Eq. (3)] best coincides with the jets scale (Fig. 6a, blue dots).

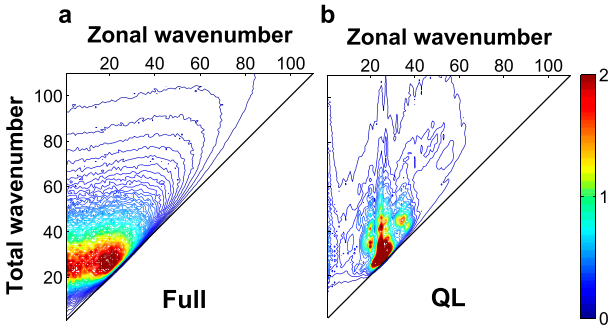

FIG. 7. The 2D spectrum, computed using spherical harmonics as basis functions (Boer and Shepherd 1983), of the barotropic EKE (10^{-2} m^2 s^{-2}) as a function of zonal and total wavenumbers in the $8\Omega_e$ simulation (a) with and (b) without eddy–eddy interactions.

supercriticality latitude (Figs. 4a,b). Consistently, in the QL simulations, stronger barotropic eddy–mean flow interactions intrude into these latitudes (Figs. 4c,d). These interactions replace the eddy–eddy interactions (which efficiently spread the input of baroclinic EKE locally in spectral space) and maintain the jets (transfer energy to the zero zonal wavenumber) at high latitudes and thus widen the jet region (Fig. 2b).

- In the full Earthlike simulation, the supercriticality latitude was found to occur poleward of the baroclinic zone. As a result, eddy–eddy interactions were found to play a negligible role in the balance (Chemke and Kaspi 2015b). Nonetheless, in the QL Earthlike simulation, an additional jet emerges at high latitudes (Fig. 2a), as in O'Gorman and Schneider (2007) and Chai and Vallis (2014). This implies that eddy–eddy interactions do have some effect on the zonal mean flow, even under Earth's parameters.
- The eddy–eddy interactions are found to have a minor effect on the meridional width of the jets through all latitudes and rotation rates (Fig. 3a). As in the full simulations in Chemke and Kaspi (2015b), the width of the jet in the QL simulations coincides with the Rhines scale through all latitudes and rotation rates (Fig. 3b). Thus, the Rhines scale also remains similar in both full and QL simulations. This congruity implies that the jet scale is not solely determined by a turbulence inverse cascade.
- The conversion scale of baroclinic to barotropic EKE does not coincide with the Rossby deformation radius for all rotation rates, both in the full and QL simulations (Figs. 4a,b and 5). It does, however, better coincide with the scale of maximum baroclinic growth, mostly poleward of the supercriticality latitude.
- The eddy–eddy interactions are found to make the flow more isotropic, as they both spread the barotropic energy along lines of constant total wavenumber (Fig. 7) and increase the energy-containing zonal wavenumber (Fig. 3c) such that it coincides with the meridional jet scale (Fig. 6a).

Acknowledgments. We thank Janni Yuval and Malte Jansen for very fruitful discussions during the preparation of this manuscript. This research has been supported by an EU-FP7 Marie Curie Career Integration Grant (CIG-304202), the Israeli Science Foundation (Grants 1310/12 and 1859/12), the Israeli Ministry of Science, a Minerva foundation grant with funding from the Federal German Ministry of Education and Research, and a Lev-Zion Ph.D. scholarship. We also acknowledge support from the Helen Kimmel Center for Planetary Science at the Weizmann Institute of Science.

REFERENCES

Ait-Chaalal, F., and T. Schneider, 2015: Why eddy momentum fluxes are concentrated in the upper troposphere. *J. Atmos. Sci.*, **72**, 1585–1604, doi:10.1175/JAS-D-14-0243.1.

Baer, F., 1972: An alternate scale representation of atmospheric energy spectra. *J. Atmos. Sci.*, **29**, 649–664, doi:10.1175/1520-0469(1972)029<0649:AASROA>2.0.CO;2.

Bakas, N. A., and P. J. Ioannou, 2014: A theory for the emergence of coherent structures in beta-plane turbulence. *J. Fluid Mech.*, **740**, 312–341, doi:10.1017/jfm.2013.663.

Barry, L., G. C. Craig, and J. Thuburn, 2002: Poleward heat transport by the atmospheric heat engine. *Nature*, **415**, 774–777, doi:10.1038/415774a.

Berloff, P., and I. Kamenkovich, 2013a: On spectral analysis of mesoscale eddies. Part I: Linear analysis. *J. Phys. Oceanogr.*, **43**, 2505–2527, doi:10.1175/JPO-D-12-0232.1.

——, and ——, 2013b: On spectral analysis of mesoscale eddies. Part II: Nonlinear analysis. *J. Phys. Oceanogr.*, **43**, 2528–2544, doi:10.1175/JPO-D-12-0233.1.

Boer, G. J., 1975: Zonal and eddy forms of the available potential energy equations in pressure coordinates. *Tellus*, **27A**, 433–442, doi:10.1111/j.2153-3490.1975.tb01697.x.

——, and T. G. Shepherd, 1983: Large-scale two-dimensional turbulence in the atmosphere. *J. Atmos. Sci.*, **40**, 164–184, doi:10.1175/1520-0469(1983)040<0164:LSTDTI>2.0.CO;2.

Chai, J., and G. K. Vallis, 2014: The role of criticality on the horizontal and vertical scales of extratropical eddies in a dry GCM. *J. Atmos. Sci.*, **71**, 2300–2318, doi:10.1175/JAS-D-13-0351.1.

Charney, J. G., 1971: Geostrophic turbulence. *J. Atmos. Sci.*, **28**, 1087–1095, doi:10.1175/1520-0469(1971)028<1087:GT>2.0.CO;2.

Chelton, D. B., R. A. Deszoeke, M. G. Schlax, E. Naggar, and N. Siwertz, 1998: Geographical variability of the first baroclinic Rossby radius of deformation. *J. Phys. Oceanogr.*, **28**, 433–460, doi:10.1175/1520-0485(1998)028<0433:GVOTFB>2.0.CO;2.

Chemke, R., and Y. Kaspi, 2015a: Poleward migration of eddy-driven jets. *J. Adv. Model. Earth Syst.*, **7**, 1457–1471, doi:10.1002/2015MS000481.

——, and ——, 2015b: The latitudinal dependence of atmospheric jet scales and macroturbulent energy cascades. *J. Atmos. Sci.*, **72**, 3891–3907, doi:10.1175/JAS-D-15-0007.1.

——, and ——, 2016: The latitudinal dependence of the oceanic barotropic eddy kinetic energy and macroturbulence energy transport. *Geophys. Res. Lett.*, doi:10.1002/2016GL067847, in press.

Constantinou, N. C., B. F. Farrell, and P. J. Ioannou, 2014: Emergence and equilibration of jets in beta-plane turbulence: Applications of stochastic structural stability theory. *J. Atmos. Sci.*, **71**, 1818–1842, doi:10.1175/JAS-D-13-076.1.

Danilov, S. D., and D. Gurarie, 2000: Quasi-two-dimensional turbulence. *Usp. Fiz. Nauk*, **170**, 921–968, doi:10.3367/UFNr.0170.200009a.0921.

Eady, E. T., 1949: Long waves and cyclone waves. *Tellus*, **1A**, 33–52, doi:10.1111/j.2153-3490.1949.tb01265.x.

Farrell, B. F., and P. J. Ioannou, 2007: Structure and spacing of jets in barotropic turbulence. *J. Atmos. Sci.*, **64**, 3652–3665, doi:10.1175/JAS4016.1.

Frierson, D. M. W., I. M. Held, and P. Zurita-Gotor, 2006: A gray-radiation aquaplanet moist GCM. Part I: Static stability and eddy scale. *J. Atmos. Sci.*, **63**, 2548–2566, doi:10.1175/JAS3753.1.

Fu, L.-L., and G. R. Flierl, 1980: Nonlinear energy and enstrophy transfers in a realistically stratified ocean. *Dyn. Atmos. Oceans*, **4**, 219–246, doi:10.1016/0377-0265(80)90029-9.

Galperin, B., S. Sukoriansky, P. Read, Y. Yamazaki, and R. Wordsworth, 2006: Anisotropic turbulence and zonal jets in rotating flows with a beta effect. *Nonlinear Processes Geophys.*, **13**, 83–98, doi:10.5194/npg-13-83-2006.

Gill, A. E., 1982: *Atmosphere–Ocean Dynamics*. International Geophysics Series, Vol. 30, Academic Press, 662 pp.

Goody, R. M., 1964: *Atmospheric Radiation*. Clarendon Press, 426 pp.

Haidvogel, D. B., and I. M. Held, 1980: Homogeneous quasi-geostrophic turbulence driven by a uniform temperature gradient. *J. Atmos. Sci.*, **37**, 2644–1660, doi:10.1175/1520-0469(1980)037<2644:HQGTDB>2.0.CO;2.

Held, I. M., 1982: On the height of the tropopause and the static stability of the troposphere. *J. Atmos. Sci.*, **39**, 412–417, doi:10.1175/1520-0469(1982)039<0412:OTHOTT>2.0.CO;2.

——, and A. Y. Hou, 1980: Nonlinear axially symmetric circulations in a nearly inviscid atmosphere. *J. Atmos. Sci.*, **37**, 515–533, doi:10.1175/1520-0469(1980)037<0515:NASCIA>2.0.CO;2.

——, and V. D. Larichev, 1996: A scaling theory for horizontally homogeneous, baroclinically unstable flow on a beta plane. *J. Atmos. Sci.*, **53**, 946–952, doi:10.1175/1520-0469(1996)053<0946:ASTFHH>2.0.CO;2.

Holloway, G., and M. C. Hendershott, 1977: Stochastic closure for nonlinear Rossby waves. *J. Fluid Mech.*, **82**, 747–765, doi:10.1017/S0022112077000962.

Huang, H. P., and W. A. Robinson, 1998: Two-dimensional turbulence and persistent jets in a global barotropic model. *J. Atmos. Sci.*, **55**, 611–632, doi:10.1175/1520-0469(1998)055<0611:TDTAPZ>2.0.CO;2.

——, B. Galperin, and S. Sukoriansky, 2001: Anisotropic spectra in two-dimensional turbulence on the surface of a rotating sphere. *Phys. Fluids*, **13**, 225–240, doi:10.1063/1.1327594.

Hunt, B. G., 1979: The influence of the earth's rotation rate on the general circulation of the atmosphere. *J. Atmos. Sci.*, **36**, 1392–1408, doi:10.1175/1520-0469(1979)036<1392:TIOTER>2.0.CO;2.

Jansen, M., and R. Ferrari, 2012: Macroturbulent equilibration in a thermally forced primitive equation system. *J. Atmos. Sci.*, **69**, 695–713, doi:10.1175/JAS-D-11-041.1.

——, and ——, 2013: Equilibration of an atmosphere by adiabatic eddy fluxes. *J. Atmos. Sci.*, **70**, 2948–2962, doi:10.1175/JAS-D-13-013.1.

Kaspi, Y., and G. R. Flierl, 2007: Formation of jets by baroclinic instability on gas planet atmospheres. *J. Atmos. Sci.*, **64**, 3177–3194, doi:10.1175/JAS4009.1.

——, and T. Schneider, 2011: Downstream self-destruction of storm tracks. *J. Atmos. Sci.*, **68**, 2459–2464, doi:10.1175/JAS-D-10-05002.1.

——, and A. P. Showman, 2015: Atmospheric dynamics of terrestrial exoplanets over a wide range of orbital and atmospheric parameters. *Astrophys. J.*, **804**, 60, doi:10.1088/0004-637X/804/1/60.

Kidston, J., and G. K. Vallis, 2010: Relationship between eddy-driven jet latitude and width. *Geophys. Res. Lett.*, **37**, L21809, doi:10.1029/2010GL044849.

Koshyk, J. N., and K. Hamilton, 2001: The horizontal kinetic energy spectrum and spectral budget simulated by a high-resolution troposphere–stratosphere–mesosphere GCM. *J. Atmos. Sci.*, **58**, 329–348, doi:10.1175/1520-0469(2001)058<0329:THKESA>2.0.CO;2.

Lambert, S. J., 1984: A global available potential energy-kinetic energy budget in terms of the two-dimensional wavenumber for the FGGE year. *Atmos.–Ocean*, **22**, 265–282, doi:10.1080/07055900.1984.9649199.

Larichev, V. D., and I. M. Held, 1995: Eddy amplitudes and fluxes in a homogeneous model of fully developed baroclinic instability. *J. Phys. Oceanogr.*, **25**, 2285–2297, doi:10.1175/1520-0485(1995)025<2285:EAAFIA>2.0.CO;2.

Lee, S., 2005: Baroclinic multiple zonal jets on the sphere. *J. Atmos. Sci.*, **62**, 2482–2498, doi:10.1175/JAS3481.1.

Lorenz, E. N., 1955: Available potential energy and the maintenance of the general circulation. *Tellus*, **7A**, 157–167, doi:10.1111/j.2153-3490.1955.tb01148.x.

Marston, J. B., 2012: Planetary atmospheres as nonequilibrium condensed matter. *Annu. Rev. Condens. Matter Phys.*, **3**, 285–310, doi:10.1146/annurev-conmatphys-020911-125114.

Merlis, T. M., and T. Schneider, 2009: Scales of linear baroclinic instability and macroturbulence in dry atmospheres. *J. Atmos. Sci.*, **66**, 1821–1833, doi:10.1175/2008JAS2884.1.

Nastrom, G. D., and K. A. Gage, 1985: A climatology of atmospheric wavenumber spectra of wind and temperature observed by commercial aircraft. *J. Atmos. Sci.*, **42**, 950–960, doi:10.1175/1520-0469(1985)042<0950:ACOAWS>2.0.CO;2.

Navarra, A., and G. Boccaletti, 2002: Numerical general circulation experiments of sensitivity to Earth rotation rate. *Climate Dyn.*, **19**, 467–483, doi:10.1007/s00382-002-0238-8.

O'Gorman, P. A., and T. Schneider, 2007: Recovery of atmospheric flow statistics in a general circulation model without nonlinear eddy–eddy interactions. *Geophys. Res. Lett.*, **34**, L22801, doi:10.1029/2007GL031779.

——, and ——, 2008a: The hydrological cycle over a wide range of climates simulated with an idealized GCM. *J. Climate*, **21**, 3815–3832, doi:10.1175/2007JCLI2065.1.

——, and ——, 2008b: Weather-layer dynamics of baroclinic eddies and multiple jets in an idealized general circulation model. *J. Atmos. Sci.*, **65**, 524–535, doi:10.1175/2007JAS2280.1.

Panetta, R. L., 1993: Zonal jets in wide baroclinically unstable regions: Persistence and scale selection. *J. Atmos. Sci.*, **50**, 2073–2106, doi:10.1175/1520-0469(1993)050<2073:ZJIWBU>2.0.CO;2.

Rhines, P. B., 1975: Waves and turbulence on a beta plane. *J. Fluid Mech.*, **69**, 417–443, doi:10.1017/S0022112075001504.

——, 1977: The dynamics of unsteady currents. *Marine Modeling*, E. D. Goldberg, Ed., The Sea—Ideas and Observations on Progress in the Study of the Seas, Vol. 6, Harvard University Press, 189–318.

——, 1979: Geostrophic turbulence. *Annu. Rev. Fluid Mech.*, **11**, 401–441, doi:10.1146/annurev.fl.11.010179.002153.

——, 1994: Jets. *Chaos*, **4**, 313–339, doi:10.1063/1.166011.

Robinson, W. A., 2006: On the self-maintenance of midlatitude jets. *J. Atmos. Sci.*, **63**, 2109–2122, doi:10.1175/JAS3732.1.

Salmon, R., 1978: Two-layer quasi-geostrophic turbulence in a simple special case. *Geophys. Astrophys. Fluid Dyn.*, **10**, 25–52, doi:10.1080/03091927808242628.

Saltsman, B., 1957: Equations governing the energetics of the larger scales of atmospheric turbulence in the domain of wave number. *J. Meteor.*, **14**, 513–523, doi:10.1175/1520-0469(1957)014<0513:EGTEOT>2.0.CO;2.

Schneider, T., and C. C. Walker, 2006: Self-organization of atmospheric macroturbulence into critical states of weak nonlinear eddy–eddy interactions. *J. Atmos. Sci.*, **63**, 1569–1586, doi:10.1175/JAS3699.1.

Shepherd, T. G., 1987a: Rossby waves and two-dimensional turbulence in a large-scale zonal jet. *J. Fluid Mech.*, **183**, 467–509, doi:10.1017/S0022112087002738.

——, 1987b: A spectral view of nonlinear fluxes and stationary–transient interaction in the atmosphere. *J. Atmos. Sci.*, **44**, 1166–1147, doi:10.1175/1520-0469(1987)044<1166:ASVONF>2.0.CO;2.

Simmons, A. J., 1974: The meridional scale of baroclinic waves. *J. Atmos. Sci.*, **31**, 1515–1525, doi:10.1175/1520-0469(1974)031<1515:TMSOBW>2.0.CO;2.

Smith, K. S., 2007: The geography of linear baroclinic instability in Earth's oceans. *J. Mar. Res.*, **65**, 655–683, doi:10.1357/002224007783649484.

——, and G. K. Vallis, 2001: The scales and equilibration of midocean eddies: Freely evolving flow. *J. Phys. Oceanogr.*, **31**, 554–571, doi:10.1175/1520-0485(2001)031<0554:TSAEOM>2.0.CO;2.

——, and ——, 2002: The scales and equilibration of midocean eddies: Forced–dissipative flow. *J. Phys. Oceanogr.*, **32**, 1699–1720, doi:10.1175/1520-0485(2002)032<1699:TSAEOM>2.0.CO;2.

Srinivasan, K., and W. R. Young, 2012: Zonostrophic instability. *J. Atmos. Sci.*, **69**, 1633–1656, doi:10.1175/JAS-D-11-0200.1.

Tobias, S. M., and J. B. Marston, 2013: Direct statistical simulation of out-of-equilibrium jets. *Phys. Rev. Lett.*, **110**, 104502, doi:10.1103/PhysRevLett.110.104502.

——, K. Dagon, and J. B. Marston, 2011: Astrophysical fluid dynamics via direct statistical simulation. *Astrophys. J.*, **727**, 127, doi:10.1088/0004-637X/727/2/127.

Vallis, G. K., and M. E. Maltrud, 1993: Generation of mean flows and jets on a beta plane and over topography. *J. Phys. Oceanogr.*, **23**, 1346–1362, doi:10.1175/1520-0485(1993)023<1346:GOMFAJ>2.0.CO;2.

Walker, C. C., and T. Schneider, 2006: Eddy influences on Hadley circulations: Simulations with an idealized GCM. *J. Atmos. Sci.*, **63**, 3333–3350, doi:10.1175/JAS3821.1.

Williams, G. P., 1978: Planetary circulations: 1. Barotropic representation of the Jovian and terrestrial turbulence. *J. Atmos. Sci.*, **35**, 1399–1426, doi:10.1175/1520-0469(1978)035<1399:PCBROJ>2.0.CO;2.

——, and J. L. Holloway, 1982: The range and unity of planetary circulations. *Nature*, **297**, 295–299, doi:10.1038/297295a0.

Zurita-Gotor, P., 2008: The sensitivity of the isentropic slope in a primitive equation dry model. *J. Atmos. Sci.*, **65**, 43–65, doi:10.1175/2007JAS2284.1.

——, and G. K. Vallis, 2009: Equilibration of baroclinic turbulence in primitive equations and quasigeostrophic models. *J. Atmos. Sci.*, **66**, 837–863, doi:10.1175/2008JAS2848.1.